Chapter 6
Large Scale Studies of Steam Methane Reforming in Packed Bed Reactor

6.1 Introduction

The steam methane reforming (SMR), which produces hydrogen, has a lot of potential for meeting the rising demand for renewable energy sources. Due to easily availability of methane, it is an economical fuel to be used in hydrogen production. [1-3] In steam reforming of methane, methane and steam react to produce syn gas. Simultaneously water gas shift reaction takes place and form carbon dioxide and hydrogen gas. [4-6] as already explained in previous chapters. As SMR is highly endothermic reaction, packed bed reactors are frequently used because of their effective mass and heat transfer properties. [7-9] To check process efficiency, safety, and catalyst stability at low temperature (500℃) for membrane reformer application, efficient large scale experiments are carried out.

An extensive investigation of the steam methane reforming in a packed bed reactor of I.D 6.35cm for 1kW membrane reformer is presented in this work at same GHSV value and keeping same residence time. The performance of a SMR nickel-based catalyst in a lab-scale packed bed reactor (I.D 11.74mm) is first assessed in the study. A controlled environment is used to evaluate conversion, selectivity, and reaction kinetics. In order to study reactor performance at greater sizes, we checked the performance of catalyst in reactor (I.D 6.35cm). [10] The analysis of catalyst particle size, and minimum fluidization velocity throughout the packed bed was defined to maintain uniform reaction conditions. Therefore, a pilot-scale reactor is built and put to the test under various parameters. The outcomes indicate that the same catalyst is showing good conversion at low temperature (500℃) with zero CO selectivity in large reactor for objective of membrane reformer

application. However, high CO selectivity can reduce the hydrogen permeability through the membranes. Higher concentrations of CO decrease hydrogen permeability across the membrane and can impact membrane reformer performance because it has been shown in the literature that CO inhibits Pd-based membranes. Since CO is produced by the principal reaction in SMR, this is crucial. For membrane reformer applications, it is therefore essential to synthesize a catalyst with low CO selectivity, low operating temperature, and short startup time. Moreover, the potential of the technique to optimize the parameters at large scale (3kW) membrane reformer as well as for high temperature is also carried out while demonstrating its viability and accuracy for future recommendations.

6.2 Experimental section

6.2.1 Catalyst Preparation

For powder catalyst pellets (3-5mm), all the catalysts were prepared by wet impregnation method. For Ni, Co, La metal doping, the precursors used were Nickel nitrate hexahydrate, cobalt nitrate hexahydrate and lanthanum nitrate hexahydrate. The total metal loading of catalysts was 10%. Al_2O_3 was used as a support. Initially, various solutions of different precursors were dissolved in a sufficient quantity of distilled water. Solution was left for vigorous stirring for at least 3 hours. After 3 hours of impregnation, the solution left for drying in oven for overnight at 120°C. After drying of samples, the sample was calcinated in muffle furnace for 6 hours at 970°C. Then 3-5mm size pellets is formed with this powder catalyst.

6.2.2 Catalyst testing in packed bed reactor

The SMR experiments were conducted in packed bed reactor of an inner diameter of 6.35cm in large reactor. A thermocouple and a pressure gauge were installed in the reactor to measure the pressure and the temperature of the catalyst bed, respectively. Before

entering the reactor, the reactant gases, methane (CH_4) and water vapor (H_2O), were preheated in separate temperature-controlled furnaces such as pre-mixer and vaporizer respectively. Before entering the reactor, the methane and inert gas nitrogen were combined in a pre-mixing chamber.

Nitrogen was first used to cleanse the reactor of any gas present in the reactor before reaction. Additionally, nitrogen is used to maintain same GHSV value as in small reactor to keep residence time same. The reactant gases (CH_4 and H_2O) were added to the reactor at the required molar ratio once the desired temperature reached. A set residence time was given for the response to continue. To ascertain the composition of the effluent gases, the product gases were collected and examined using a gas chromatograph outfitted with a thermal conductivity detector (TCD).

Then minimum fluidization velocity is calculated so that catalyst does not fluidize. At the same residence time as in small reactor, this catalyst is tested in scale up reactor to compare the results. Moreover, in addition to this, various parameters such as catalyst flow rate, effect of high temperature, W/F, GHSV, effect of pressure are also studied.

Fig. 6.1 Experimental set up of scale up reactor of I.D 6.35cm

Table 6.1 Specifications for small and scale up reactor

Parameters	Small reactor	Scaleup 1kW	Scaleup 3kW
Reactor Diameter	11.74mm	6.35cm	6.35cm
L_C/D	1.2	3.4	3.4
L_c/D_P	58.3	55.1	55.1
D/D_P	48.8	21.2	21.2
GHSV (Same)	**10,739 h^{-1}**	**10,739 h^{-1}**	**10,739 h^{-1}**
Catalyst size	180-300 µm	3-5mm	3-5mm
Type of particle	Geldart group B	Geldart group D	Geldart group D

All experiments are performed at same GHSV value in large reactor as in small reactor

The Table 6.1 compares the operational parameters for steam methane reforming using a Ni-Co-La/Al_2O_3 catalyst across three reactor configurations: a small reactor (inner diameter 11.74 mm) and large reactor for 1 kW and 3 kW (both with an inner diameter of 6.35 cm). The small reactor uses smaller catalyst particles (180–300 μm) classified as Geldart Group B, while the large reactor uses larger particles (3–5 mm) classified as Geldart Group D, which are more suitable for larger systems to reduce pressure drop and improve fluid dynamics. The length-to-diameter ratio (Lc/D) increases significantly from 1.2 in the small reactor to 3.4 in the scale-up reactors, ensuring same residence time for reactions despite the larger diameter. Similarly, the length-to-particle size ratio (Lc/D_p) and diameter-to-particle size ratio (D/D_p) are adjusted in the large reactor to accommodate the larger catalyst particles, maintaining consistent flow conditions. Gas hourly space velocity (GHSV) remains constant at 10,739 h^{-1} across all configurations, ensuring uniform reaction conditions.

6.3 Results and Discussion

6.3.1 Effect of temperatures

Effect of various temperatures in scale up reactor

The graph shows how well a Ni-Co-La/Al_2O_3 catalyst performs steam methane reforming at temperatures ranging from 500°C to 800°C in order to generate 1 kW of electricity. In line with the endothermic nature of the process, which favors higher temperatures, it shows that methane conversion much improves with increasing temperature [11-16]. Performance gradually improves as the temperature rises from 650°C to 750°C, with increased conversion. The catalyst exhibits its maximal activity at 800°C, where it attains near-complete methane conversion. But high temperature reaction is also associated with high CO selectivity that limit the application of membrane reformer. On the other hand, the

objective of this study is to study the results at low temperature (500°C) for the application of membrane reformer.

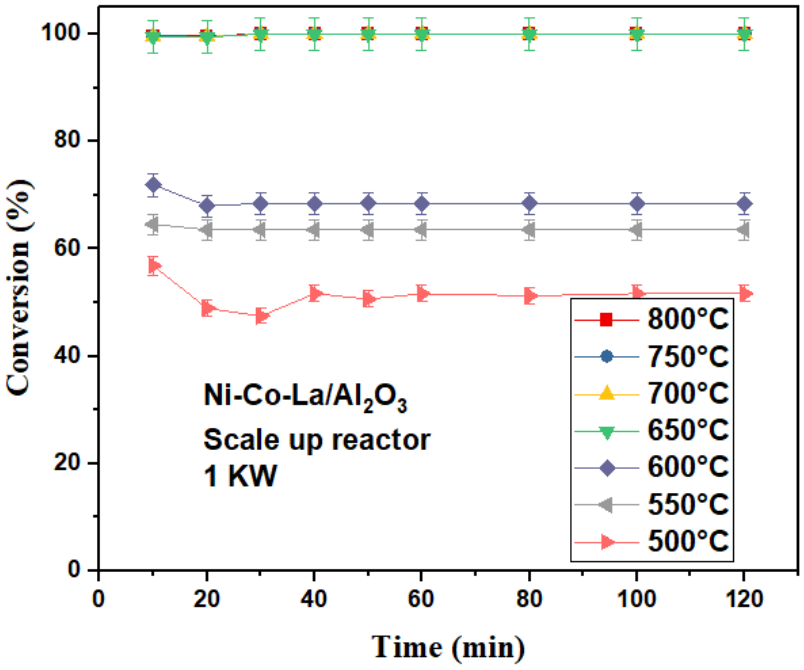

Fig. 6.2 Conversion vs time graph of Ni-Co-La/Al_2O_3 catalyst for all temperatures for 1 kW system

Effect of temperature on CO and CO_2 selectivity

The graphs show the trends in CO and CO_2 selectivity for the Ni-Co-La/Al_2O_3 catalyst during steam methane reforming throughout a temperature range of 500°C to 800°C. Zero CO selectivity is also obtained in large reactor at low temperature (500°C) at same GHSV value as shown in Fig 6.3(a). The reverse water-gas shift process ($CO_2 + H_2 \rightarrow CO + H_2O$) or incomplete reforming reactions are probably the causes of the relatively high CO selectivity at high temperatures (650°C to 800°C). [17-19] Nevertheless, CO selectivity dramatically increases as the temperature rises (from 650°C to 800°C), indicating that high temperatures promote the reverse water-gas shift process ($CO + H_2O \rightarrow CO_2 + H_2$) and lead to more thorough methane reforming. On the other hand, the CO_2 selectivity shows that

CO_2 selectivity rises with low temperature. Because side reactions that produce CO predominate at high temperatures, CO_2 selectivity is low. Selectivity for CO_2 decreases dramatically with high temperature, indicating the catalyst improved capacity to drive the water-gas shift reaction and transform CO into CO_2. Therefore, it can be concluded that Ni-Co-La/Al_2O_3 catalyst is well suitable even for large scale systems at low temperature (500°C) to fulfill the objective of this study by getting maximum conversion (almost 50%) and zero CO selectivity for the membrane reformer application. However, high temperature is not required for membrane reformer application even though effect of high temperature is also seen in large reactors for the future recommendations.

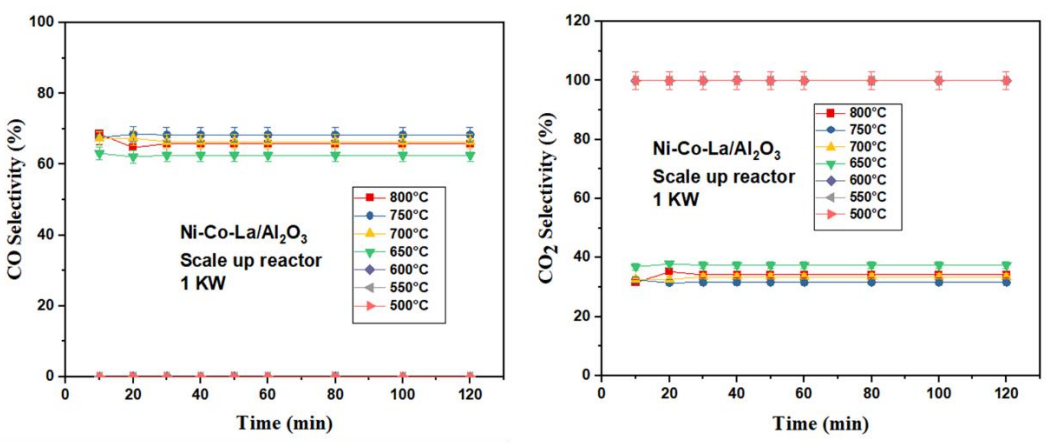

Fig. 6.3 Ni-Co-La/Al_2O_3 catalyst for all temperatures for 1 kW system (a) CO selectivity (b) CO_2 selectivity vs time

6.3.2 Effect of various W/F in large reactor

The Fig. 6.4 shows the Ni-Co-La/Al_2O_3 catalyst methane conversion as a function of time at various weight-to-flow (W/F) ratios during steam methane reforming. The catalyst weight (W) divided by the methane molar flow rate (F) is known as the W/F ratio. Over

time, methane conversion is almost constant at all W/F values as metal loading was 10%. The stable and effective reforming is made possible by a catalyst weight that is adequate in relation to the methane flow rate. [20-24]

The catalyst sustains its activity throughout the test period without experiencing appreciable deactivation, as evidenced by the conversion stability over time at all W/F ratios. The catalyst is also tested in this experiment at same W/F 26.8 kg_{cat} s/mol as used in small reactor. Almost same conversion is obtained for all W/F values as represented in Fig. 6.4.

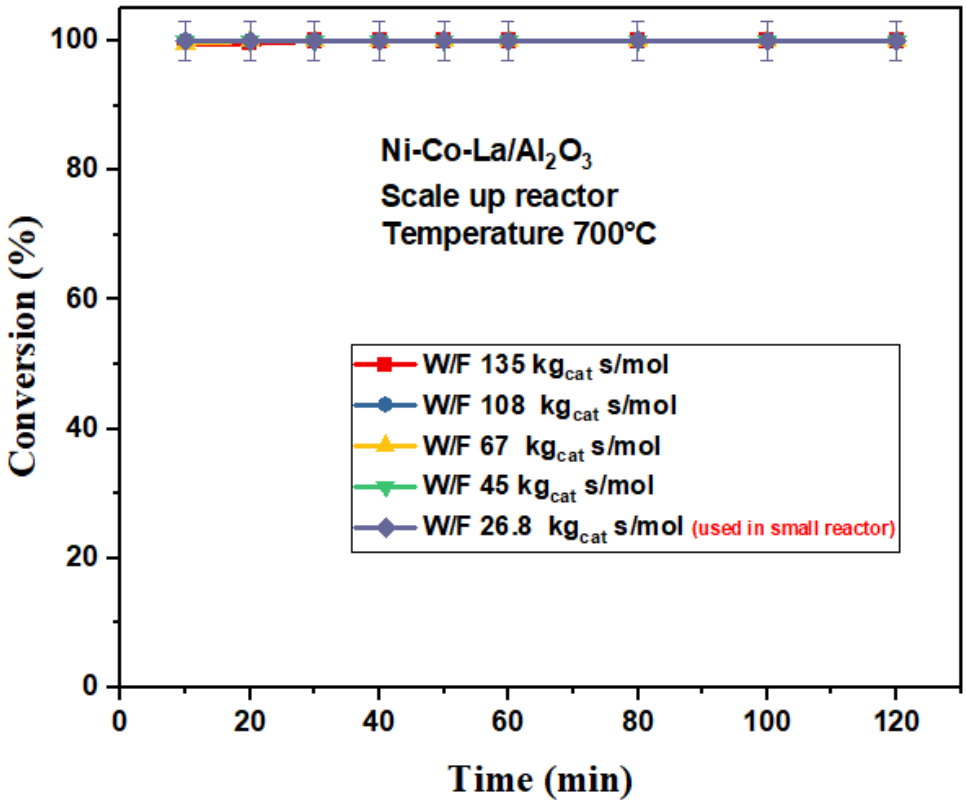

Fig. 6.4 Conversion vs time graph of Ni-Co-La/Al_2O_3 catalyst for W/F values

Effect of W/F on CO and CO_2 selectivity

The Fig. 6.5 show how the Ni-Co-La/Al_2O_3 catalyst CO and CO_2 selectivity changed over time at various weight-to-flow (W/F) ratios during steam methane reforming. Selectivity

steadily declines as W/F ratios rise in the CO selectivity graph. CO selectivity stays lower throughout the reaction for higher W/F values, such 135 and 108 $kg_{cat}s/mol$, indicating more efficient water-gas shift reactions and improved CO conversion to CO_2. CO selectivity, on the other hand, is higher at lower W/F ratios, such as 26.8 $kg_{cat}s/mol$, suggesting less effective conversion because of either insufficient catalytic activity. In small reactor, CO selectivity obtained with Ni-Co-La/Al_2O_3 is almost 22% at 700°C and zero at 500°C. Whereas, in large reactor, it increased to almost 80% CO selectivity at same W/F 26.8 $kg_{cat}s/mol$ as used in same reactor, at high temperature 800°C. The CO_2 selectivity graph, on the other hand, exhibits an inverse trend, with greater W/F ratios translating into higher CO_2 selectivity. It can be seen CO selectivity is getting increased in large reactor at higher temperature (800°C) at all W/F values. Therefore, it can be concluded that this catalyst is suitable in large reactor at low temperature (500°C) for membrane reformer application as illustrated in Fig. 6.3(a). [25-27]

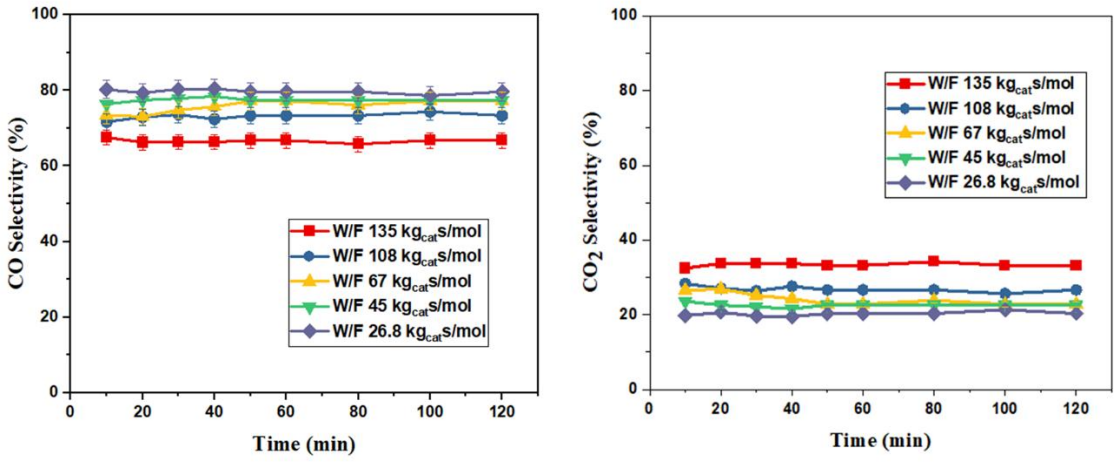

Fig. 6.5 Ni-Co-La/Al_2O_3 catalyst for W/F for 1 kW system (a) CO selectivity (b) CO_2 selectivity

6.4 Large scale studies to 3kW

Conversion

The Ni-Co-La/Al_2O_3 catalysts performance during steam methane reforming to produce hydrogen at power outputs of 3 kW is shown in the Fig. 6.6. The methane flow rate was modified to correspond with the hydrogen demand required to produce 3kW membrane reformer at W/F 42.6 kg $_{cat}$s/mol. The catalyst capacity to sustain high activity under a range of operating settings is demonstrated by the results, which demonstrate that the methane conversion efficiency is constant across at 3kW for the same GHSV value.

[28-30]

The methane flow rate increases proportionately as the power need rises to 3 kW, by keeping GHSV value same for having same residence time. This illustrates the Ni-Co-La/Al_2O_3 catalyst results good in large reactor, as it can manage higher feed rates without sacrificing reaction efficiency. Experiments are already performed for different W/F values as represented in Fig. 6.5. The CO selectivity obtained for 3kW power system at W/F 42.6 kg_{cat}s/mol is almost same as W/F value data in Fig. 6.5 Furthermore, the steady trend in methane conversion at 3kW indicates that the increased methane feed rates are not overwhelming the catalyst active sites. It is appropriate for changing power generating needs because of its robustness, which guarantees consistent hydrogen production. The catalyst capacity to function well in these circumstances also demonstrates its strong resistance to carbon deposition, effective active metal dispersion, and thermal stability all of which are essential for long-term and realistic uses in the production of hydrogen for electricity. Overall, the findings support the high effectiveness and versatility of the Ni-Co-La/Al_2O_3 catalyst, which makes it a good catalyst for large scale methane reforming procedures that can be adjusted to meet power generating atleast upto 3kW.

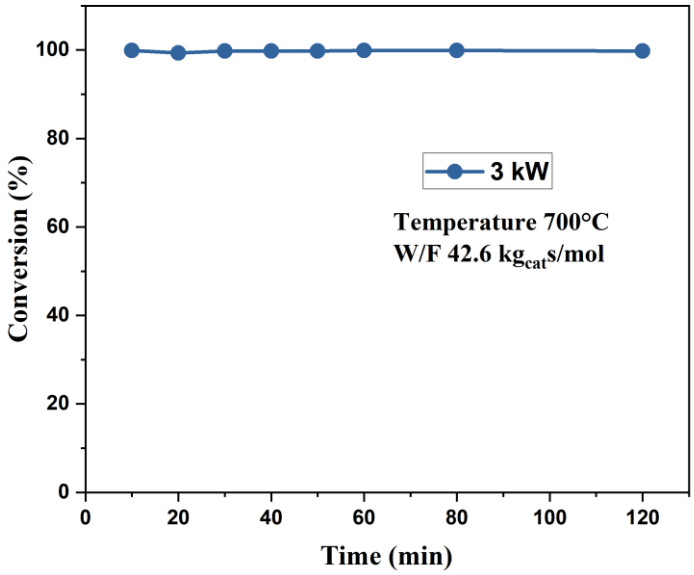

Fig. 6.6 Conversion vs time graph of Ni-Co-La/Al_2O_3 catalyst for 3kW system at 700°C

CO Selectivity

The Ni-Co-La/Al_2O_3 catalyst performance for steam methane reforming is shown in the Fig. 6.7 at power output level 3 kW. The methane flow rate in this investigation was meticulously modified to satisfy the unique energy requirements of energy level. A direct and predictable relationship between fuel intake and energy production is demonstrated by the fact that, as anticipated, an increase in power output results in a corresponding rise in the methane flow rate. Even when the methane flow rate is raised, the catalyst performance does not noticeably deteriorate, but the CO selectivity is increased for higher power output. This constancy highlights how resilient the Ni-Co-La/Al_2O_3 catalyst is to sustaining high activity and conversion efficiency even in the face of fluctuating operating circumstances but for high power output such as 3kW, it increased.

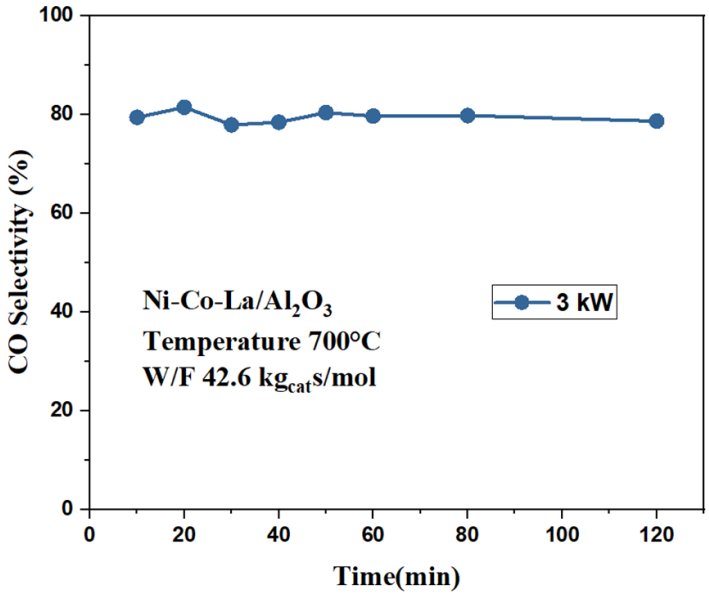

Fig. 6.7 Ni-Co-La/Al_2O_3 catalyst for 3kW system for CO selectivity

6.5 Effect of pressure

The Fig. 6.8 can be used to study how pressure affects steam methane reforming with a Ni-Co-La/Al_2O_3 catalyst in a packed bed reactor with an inner diameter of 6.35 cm. The methane conversion varies slightly as the pressure rises from 0 to 3 bar. The catalyst activity guarantees consistent performance across pressures, even though increasing pressure typically lowers the equilibrium conversion because of the methane reforming reaction reverse shift in equilibrium (as it creates more moles of gas).

CO and CO_2 selectivity: Throughout the pressure range, there are minor variations in the selectivity for CO and CO_2. Because the water-gas shift process is less favorable at greater pressures, CO production may somewhat increase, but CO_2 stays rather steady.

Despite less-than-ideal thermodynamic circumstances at higher pressures, the catalyst efficiently drives the steam methane reforming reaction, as evidenced by its strong performance at all measured pressures. The steam methane reforming reaction kinetics and thermodynamics are influenced by pressure. The Ni-Co-La/Al_2O_3 catalyst exhibits steady performance, making it appropriate for operations across a range of pressures in the packed

bed reactor, even if increased pressure somewhat impairs methane conversion because of equilibrium restrictions.

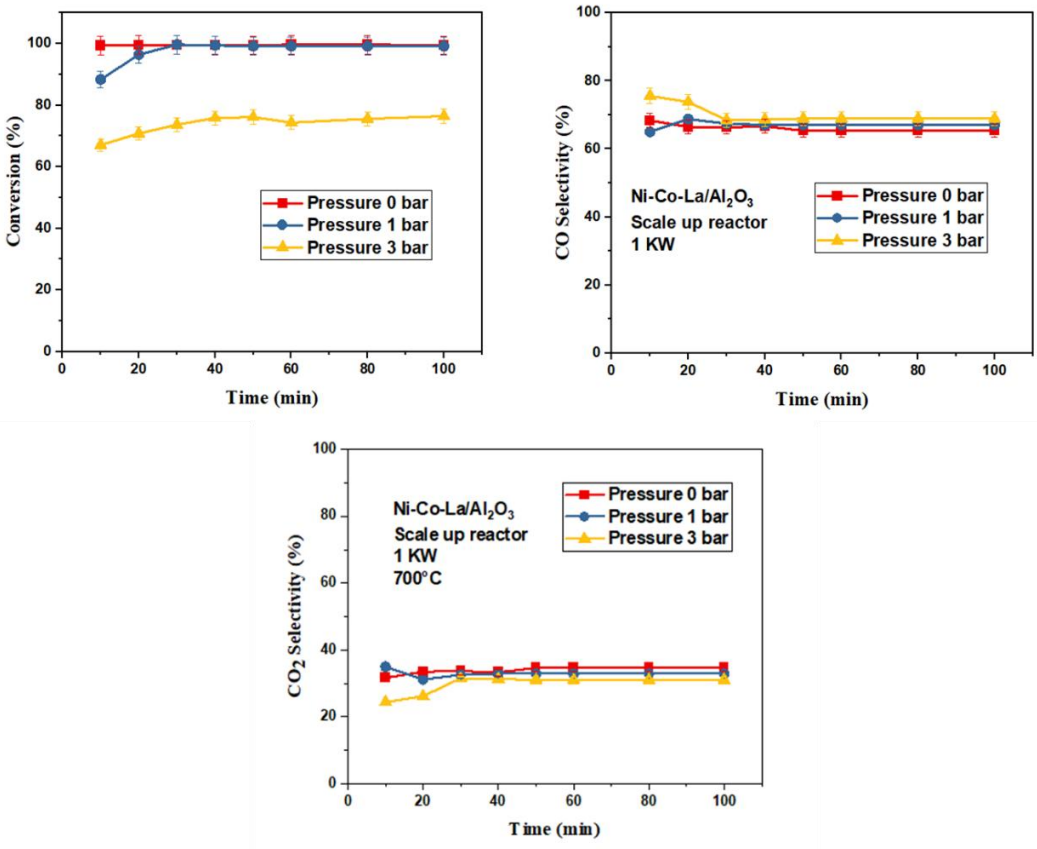

Fig. 6.8 Conversion vs time graph of Ni-Co-La/Al_2O_3 catalyst for all pressures for 1 kW system at 700℃ (a) Conversion (b) CO selectivity (c) CO_2 selectivity

6.6 Characterization results

TEM

The structural and morphological alterations in Ni-Co-La/Al_2O_3 catalyst powders employed in a 1 kW steam methane reforming system are depicted by the TEM investigation as shown in Fig. 6.9. The TEM picture (a) shows that the fresh catalyst (a-c) has well-dispersed particles with a rather uniform size distribution. A highly crystalline structure is shown by the brilliant, distinct diffraction rings in the accompanying SAED image (b). The homogeneity of the catalyst particles is seen in the narrow particle size distribution (c). The spent catalyst exhibits a wider size distribution and higher particle

agglomeration in the TEM image following usage in the small reactor (d-f), indicating sintering or particle growth. The structural and morphological alterations in Ni-Co-La/Al_2O_3 catalyst powders employed in a 1 kW steam methane reforming system are depicted by the TEM investigation. The TEM picture shows that the fresh catalyst (a-c) has well-dispersed particles with a rather uniform size distribution. A highly crystalline structure is shown by the brilliant, distinct diffraction rings in the accompanying SAED image (b). The homogeneity of the catalyst particles is seen in the narrow particle size distribution (c). The spent catalyst exhibits a wider size distribution (f) and higher particle agglomeration in the TEM image (d) following usage in the small reactor (d-f), indicating sintering or particle growth. [31-33]

The spent Ni-Co-La/Al_2O_3 catalyst utilized in a steam methane reforming process in a scaled-up reactor is depicted in the TEM image (6.35 cm i.d.) as represented in (g). Clusters of nanoparticles are visible in the image; the oxide support (AlO_3 or La-doped alumina) is represented by brighter areas, while the darker parts most likely belong to metallic phases (Ni, Co). The particles' agglomeration and potential size expansion point to sintering, a frequent deactivation mechanism that results in a smaller active surface area at high reforming temperatures. Although more research is necessary to confirm, the lack of distinct carbon layers suggests that there is little to no coke deposition evident at this magnification. Catalyst deactivation may also result from modifications in the way the active metal phases interact with the mixed oxide support.

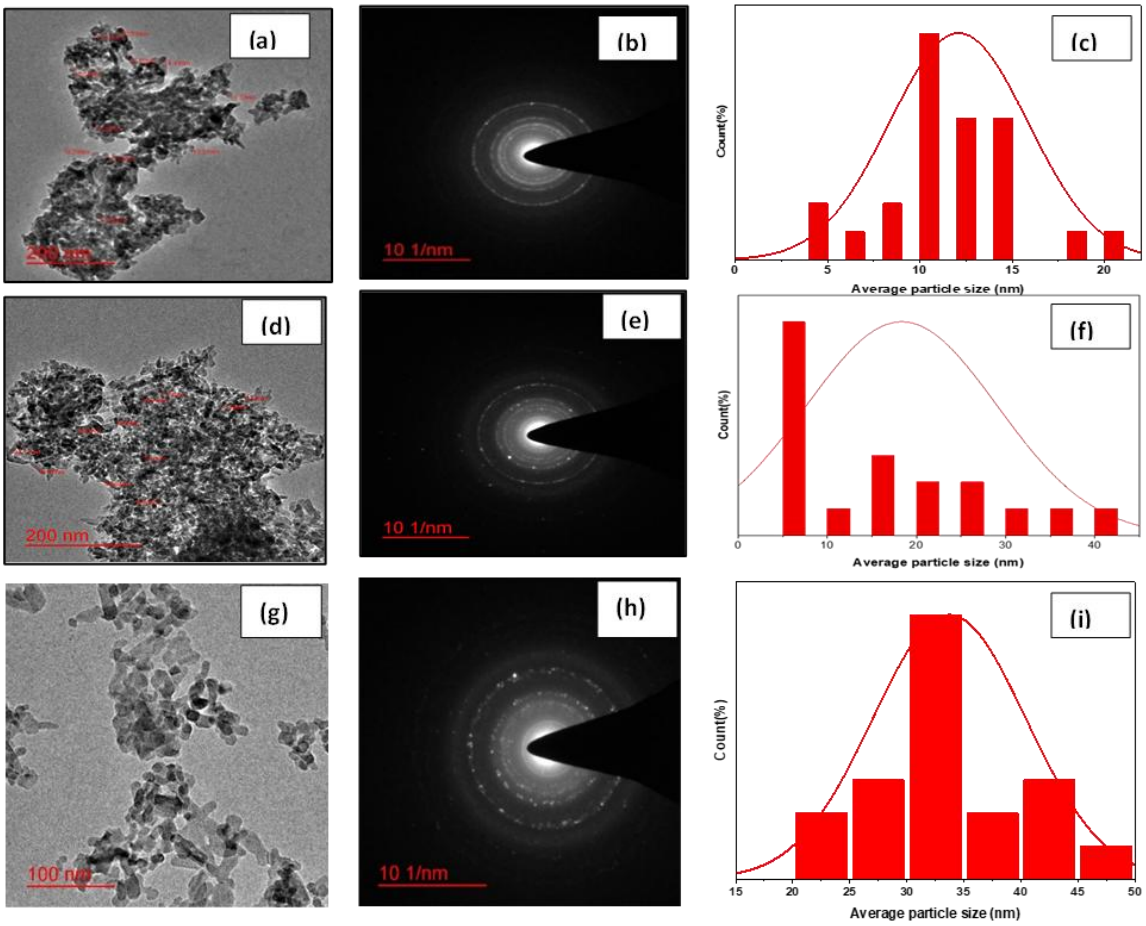

Fig. 6.9 TEM image of Ni-Co-La/Al_2O_3 catalyst powder pellets for 1 kW system (a-c) Fresh catalyst (d-f) Spent catalyst after small reactor of I.D 11.74mm (g-i) Spent catalyst after scale up reactor of I.D 6.35cm

BET

The surface area, pore volume, pore diameter, and isotherm type of the catalysts used in steam methane reforming are highlighted in the table along with their other physicochemical characteristics. With a Type 4 isotherm that indicates mesoporous structures, θ-Alumina, the base material, has a surface area of 134 m^2/g, a pore volume of 0.243 cm^3/g, and a pore diameter of 6.941 nm. With an active metal combination, the new Ni-Co-La/Al_2O_3 catalyst exhibits lower pore volume (0.143 cm^3/g) and pore diameter (22.31 nm), but a lower surface area (83.442 m^2/g), most likely as a result of metal

deposition changing the textural characteristics. The spent catalysts exhibit noticeable degradation following seven cycles in various reactor sizes with steam methane reforming at 800°C. [34,35]

Table 6.2 BET surface area, pore volume, pore diameter and type of isotherm of catalysts

Catalyst	**Surface Area m^2/g**	**Pore Volume cm^3/g**	**Pore Diameter (nm)**	**Type of isotherm**
θ- Alumina	134	0.243	6.94	Type 4
Fresh Ni-Co-La/Al_2O_3	83.4	0.143	22.31	Type 4
Spent Ni-Co-La/Al_2O_3 (Small reactor). After 800°C reaction	77.02	0.105	19.7	Type 4
Spent Ni-Co-La/Al_2O_3 (Scale-up reactor). After 800°C reaction	71.765	0.092	17.4	Type 4

The spent catalyst after large reactor exhibits a reduced pore volume of 0.092 cm^3/g, a pore width of 17.4 nm, and a surface area of 71.765 m^2/g in small reactor. Despite the structural alterations, the Type 4 isotherm remains constant across all samples, indicating that mesoporosity has been maintained. The findings highlight how high-temperature reactions and cycling affect the textural characteristics of the catalyst, which can affect how well it performs and how long it lasts in steam methane reforming.

SEM

The surface morphology of Ni-Co-La/Al_2O_3 catalyst powders for a 1 kW steam methane reforming system is depicted in the SEM Fig. 6.10, which contrast the spent catalyst following use in the scaled-up reactor (b) with the fresh catalyst (a).

The fresh catalyst (a) exhibits a porous structure and evenly distributed particles of comparatively uniform sizes on its surface. High surface area is indicated by this shape, which is advantageous for catalytic activity. Effective contact with reactants is ensured by the unique appearance of the particles and their low aggregation. The spent catalyst (b), on the other hand, exhibits notable morphological changes. There is greater particle agglomeration and the surface looks more compact. The spent catalyst has less pronounced particle boundaries, which may indicate sintering or fusion of particles throughout the reaction process. These alterations are probably the consequence of the scaled-up reactor extended operating conditions and exposure to high temperatures. [36,37].

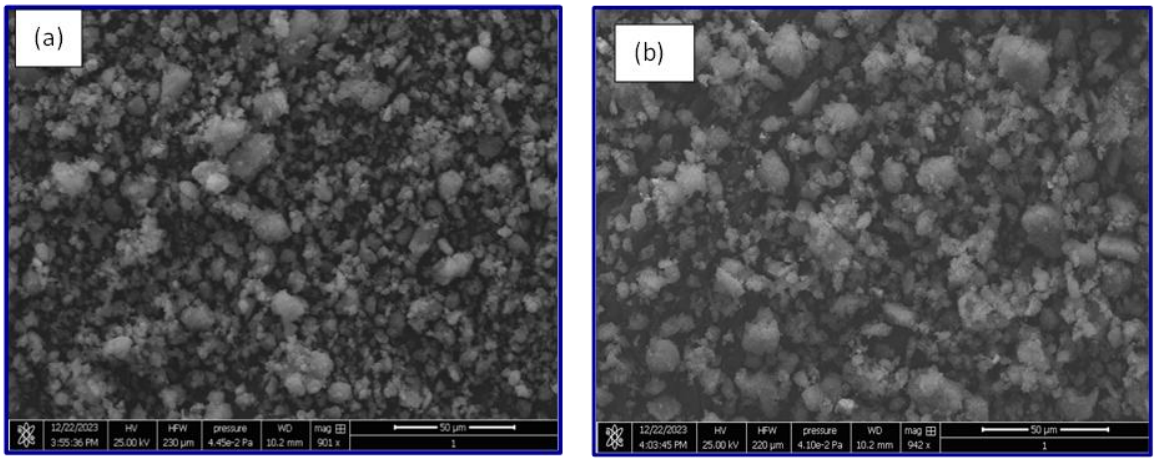

Fig. 6.10 Ni-Co-La/Al_2O_3 catalyst powder pellets for 1 kW system (a) Fresh catalyst (b) Spent catalyst after scale up reactor

Overall, the SEM research shows how the catalyst surface area and catalytic efficiency can be adversely affected by structural deterioration during use. Sintering and particle development, which are frequently linked to catalyst deactivation during high-temperature processes like steam methane reforming, are compatible with the observed morphological changes.

6.7 Conclusions

The current work focused on the crucial elements of experiments in the large reactor (I.D 6.35cm) for steam methane reforming (SMR) reactions employing a packed bed reactor. Additionally, it was observed that using a nickel-based catalyst promoted with cobalt and lanthanum greatly increased catalytic activity and stability. Improved methane conversion, and low CO selectivity at low temperature were all observed by the promoted catalyst, all of which are essential for catalytic performance for large scale for membrane reformer application.

Finally, the results of this work highlighted the trimetallic catalyst activity in packed bed reactor for large reactor where properties are already optimized in small scale reactor for membrane reformer application to get maximum conversion and zero CO selectivity at low temperature (500°C). Then, we optimized and tested the same catalyst in upscale reactor of I.D 6.35cm. The catalytic activity in upscale reactor is same as obtained in small reactor of I.D 11.74mm for low temperature (500°C). It can be concluded that this catalyst can be used in large reactor for membrane reformer application at low temperature.

References

1. Zhang X, Jin H, 2013. Thermodynamic analysis of chemical- looping hydrogen generation. *Appl Energy*. 112, 800–7
2. Van Hook, J. P. (1980). Methane-steam reforming. *Catalysis Reviews—Science and Engineering*, 21(1), 1-51.
3. Iulianelli, A., Liguori, S., Wilcox, J., Basile, A. (2016). Advances on steam methane reforming to produce hydrogen through membrane reactors technology: A review. *Catalysis Reviews*, 58(1), 1-35.
4. Ghoneim SA, El-Salamony RA, El-Temtamy SA, 2016. Review on innovative catalytic reforming of natural gas to syngas. *World J Eng Technol.* 4, 116.
5. Xu, J., Froment, G. F. (1989). Steam methane reforming, methanation and water-gas shift: I. Intrinsic kinetics. *AIChE journal*, 35(1), 88-96.
6. Zhang, H., Sun, Z., Hu, Y. H. (2021). Steam reforming of methane: Current states of catalyst design and process upgrading. *Renewable and Sustainable Energy Reviews*, 149, 111330.
7. Chompupun, T., Limtrakul, S., Vatanatham, T., Kanhari, C., Ramachandran, P. A. (2018). Experiments, modeling and scaling-up of membrane reactors for hydrogen production via steam methane reforming. *Chemical Engineering and Processing-Process Intensification*, 134, 124-140.
8. Ganguli, A., Bhatt, V. (2023). Hydrogen production using advanced reactors by steam methane reforming: a review. *Frontiers in Thermal Engineering*, 3, 1143987.
9. Gallucci, F., Comite, A., Capannelli, G., Basile, A. (2006). Steam reforming of methane in a membrane reactor: an industrial case study. *Industrial & engineering chemistry research*, 45(9), 2994-3000.
10. Baudh, A., Sharma, R., Sharma, S., Kumar Upadhyay, R. (2024). Effect of Lanthanum

and Iron Doping on Nickel-Based Alumina and Ceria Supported Catalysts for Steam Reforming of Methane. *ChemistrySelect,* 9(19), e202401393.

11. Matsumura, Y., Nakamori, T. (2004). Steam reforming of methane over nickel catalysts at low reaction temperature. *Applied Catalysis A: General*, 258(1), 107-114.
12. LeValley, T. L., Richard, A. R., Fan, M. (2015). Development of catalysts for hydrogen production through the integration of steam reforming of methane and high temperature water gas shift. *Energy*, 90, 748-758.
13. Roh, H. S., Jun, K. W. (2009). Low temperature steam methane reforming for hydrogen production for fuel cells. *Bull Korean Chem Soc*, 30, 153-6.
14. Angeli, S. D., Turchetti, L., Monteleone, G., Lemonidou, A. A. (2016). Catalyst development for steam reforming of methane and model biogas at low temperature. *Applied Catalysis B: Environmental*, 181, 34-46.
15. Nieva, M. A., Villaverde, M. M., Monzón, A., Garetto, T. F., Marchi, A. J. (2014). Steam-methane reforming at low temperature on nickel-based catalysts. *Chemical Engineering Journal*, 235, 158-166.
16. Khzouz, M., Gkanas, E. I. (2017). Experimental and numerical study of low temperature steam methane reforming for hydrogen production. *Catalysts*, 8(1), 5.
17. Choudhary, T. V., Goodman, D. W. (2000). CO-free production of hydrogen via stepwise steam reforming of methane. *Journal of catalysis*, 192(2), 316-321.
18. Venkataraman, K., Wanat, E. C., Schmidt, L. D. (2003). Steam reforming of methane and water-gas shift in catalytic wall reactors. *AIChE Journal*, 49(5), 1277-1284.
19. Amjad, U. E. S., Vita, A., Galletti, C., Pino, L., Specchia, S. (2013). Comparative study on steam and oxidative steam reforming of methane with noble metal catalysts. *Industrial & Engineering Chemistry Research*, 52(44), 15428-15436.
20. Serrano-Lotina, A., Daza, L. (2014). Influence of the operating parameters over dry

reforming of methane to syngas. *International Journal of Hydrogen Energy*, 39(8), 4089-4094.

21. Hou, K., Hughes, R. (2001). The kinetics of steam methane reforming over a Ni/α-Al_2O_3 catalyst. *Chemical Engineering Journal*, 82(1-3), 311-328.
22. Shu, J., Grandjean, B. P., Kaliaguine, S. (1994). Steam methane reforming in asymmetric Pd-and Pd-Ag/porous SS membrane reactors. *Applied Catalysis A: General*, 119(2), 305-325.
23. Naseri, A. T., Peppley, B. A., Pharoah, J. G. (2015). A systematic parametric study on the effect of a catalyst coating microstructure on its performance in steam methane reforming. *International Journal of Hydrogen Energy*, 40(46), 16086-16095.
24. Wang, Y., Wang, H., Dam, A. H., Xiao, L., Qi, Y., Niu, J., Chen, D. (2020). Understanding effects of Ni particle size on steam methane reforming activity by combined experimental and theoretical analysis. *Catalysis Today*, 355, 139-147.
25. Purnama, H., Ressler, T., Jentoft, R. E., Soerijanto, H., Schlögl, R., Schomäcker, R. (2004). CO formation/selectivity for steam reforming of methanol with a commercial CuO/ZnO/Al_2O_3 catalyst. *Applied Catalysis A: General*, 259(1), 83-94.
26. Profeti, L. P., Ticianelli, E. A., Assaf, E. M. (2008). Co/Al_2O_3 catalysts promoted with noble metals for production of hydrogen by steam methane reforming. *Fuel*, 87(10-11), 2076-2081.
27. Sahoo, D. R., Vajpai, S., Patel, S., Pant, K. K. (2007). Kinetic modeling of steam reforming of ethanol for the production of hydrogen over Co/Al_2O_3 catalyst. *Chemical Engineering Journal,* 125(3), 139-147.
28. Tacchino, V., Costamagna, P., Rosellini, S., Mantelli, V., Servida, A. (2022). Multi-scale model of a top-fired steam methane reforming reactor and validation with industrial experimental data. *Chemical Engineering Journal*, 428, 131492.

29. Gallucci, F., Comite, A., Capannelli, G., Basile, A. (2006). Steam reforming of methane in a membrane reactor: an industrial case study. *Industrial & engineering chemistry research*, 45(9), 2994-3000.

30. Bhat, S. A., Sadhukhan, J. (2009). Process intensification aspects for steam methane reforming: an overview. *AIChE Journal*, 55(2), 408-422.

31. Boukha, Z., Jiménez-González, C., de Rivas, B., González-Velasco, J. R., Gutiérrez-Ortiz, J. I., López-Fonseca, R. (2014). Synthesis, characterization and performance evaluation of spinel-derived Ni/Al_2O_3 catalysts for various methane reforming reactions. *Applied Catalysis B: Environmental*, 158, 190-201.

32. Morales-Cano, F., Lundegaard, L. F., Tiruvalam, R. R., Falsig, H., Skjøth-Rasmussen, M. S. (2015). Improving the sintering resistance of Ni/Al_2O_3 steam-reforming catalysts by promotion with noble metals. *Applied Catalysis A: General*, 498, 117-125.

33. Ewbank, J. L., Kovarik, L., Diallo, F. Z., Sievers, C. (2015). Effect of metal–support interactions in Ni/Al_2O_3 catalysts with low metal loading for methane dry reforming. *Applied Catalysis A: General*, 494, 57-67.

34. Zarei-Jelyani, F., Salahi, F., Farsi, M., Rahimpour, M. R. (2022). Synthesis and application of Ni-Co bimetallic catalysts supported on hollow sphere Al_2O_3 in steam methane reforming. *Fuel*, 324, 124785.

35. Aker, V., Ayas, N. (2023). Boosting hydrogen production by ethanol steam reforming on cobalt-modified $Ni-Al_2O_3$ catalyst. *International Journal of Hydrogen Energy*, 48(60), 22875-22888.

36. You, X., Wang, X., Ma, Y., Liu, J., Liu, W., Xu, X., Chen, X. (2014). $Ni-Co/Al_2O_3$ bimetallic catalysts for CH_4 steam reforming: elucidating the role of Co for improving coke resistance. *ChemCatChem*, 6(12), 3377-3386.

37. Ergazieva, G. E., Makayeva, N., Shaimerden, Z., Soloviev, S. O., Telbayeva, M.,

Akkazin, E., Ahmetova, F. (2022). Catalytic decomposition of Methane to hydrogen over Al_2O_3 supported mono-and bimetallic catalysts. *Bulletin of Chemical Reaction Engineering & Catalysis*, 17(1), 1-12.